SUPPORT INFORMATION

The effects of chemical and thermal exfoliation on the physico-chemical and optical properties of carbon nitrides

Tayline V. de Medeiros,[a]* Arilza O. Porto,[b] Hudson A. Bicalho,[a] Juan C. González,[c] Rafik Naccache[a] and Ana Paula C. Teixeira[b]*

[a.] *Department of Chemistry and Biochemistry and the Centre for NanoScience Research, Concordia University, Montreal, QC, Canada, H4B 1R6*

Quebec Centre for Advanced Materials, Department of Chemistry and Biochemistry, Concordia University, Montreal, QC, H4B 1R6, Canada

[b.] *Department of Chemistry, Universidade Federal de Minas Gerais, UFMG, 31270901, MG, Brazil*

[c.] *Department of Physics, Universidade Federal de Minas Gerais, UFMG, 31270901, MG, Brazil.*

*tayline.medeiros@concordia.ca
*anapct@ufmg.br

1. Atomic Force Microscopy (AFM) 2
2. X-Ray Diffraction (XRD) 3
3. Fluorescence Emission 4
4. Time-resolved Fluorescence 5
6. Transmission Electronic Microscopy 6
7. Thermogravimetric Analysis 7
8. Elemental Analysis 8
9. Fourier-Transform Infrared Spectroscopy 9
10. Tauc Plot 10
11. Fluorescence Emission of the Dicyandiamide and Urea-based Materials 11

1. Atomic Force Microscopy (AFM)

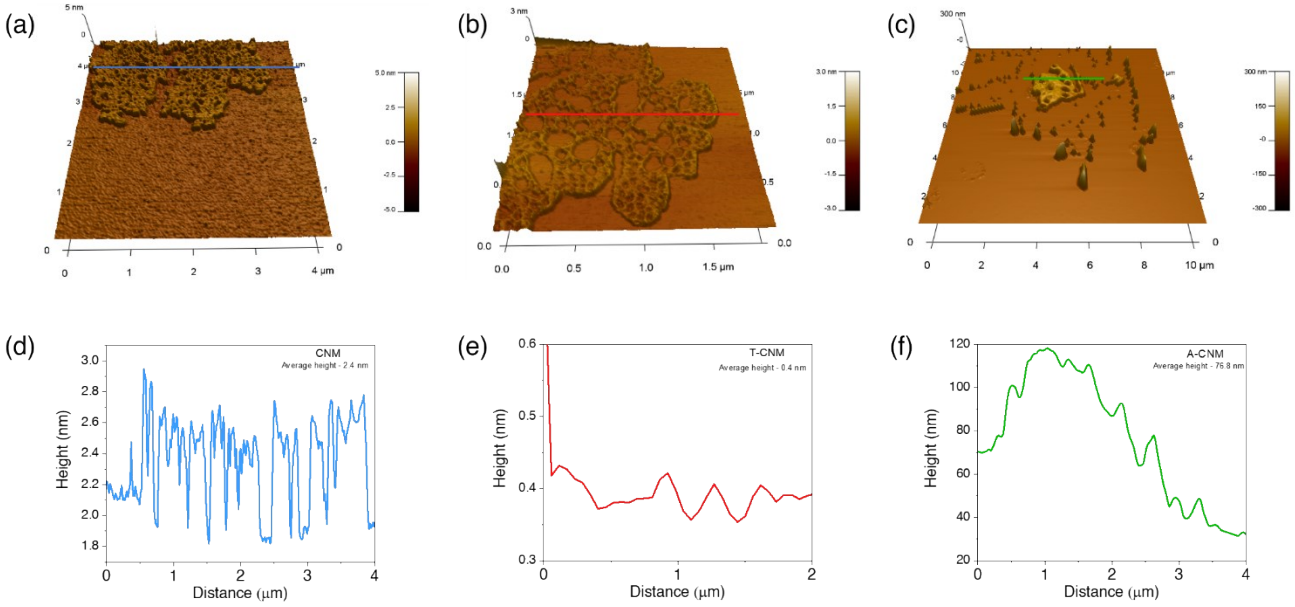

Figure S1: 3D-AFM images and height profiles along the line for CNM (a, d - average height 2.4 nm), T-CNM (b,e - average height 0.4 nm) and A-CNM (c,f - average height 76.8 nm). These findings indicate that the thermal treatment delaminates the bulk material, forming structures with reduced average height, while the acid treatment leads to the formation of smaller structures with increased thickness.

2. X-Ray Diffraction (XRD)

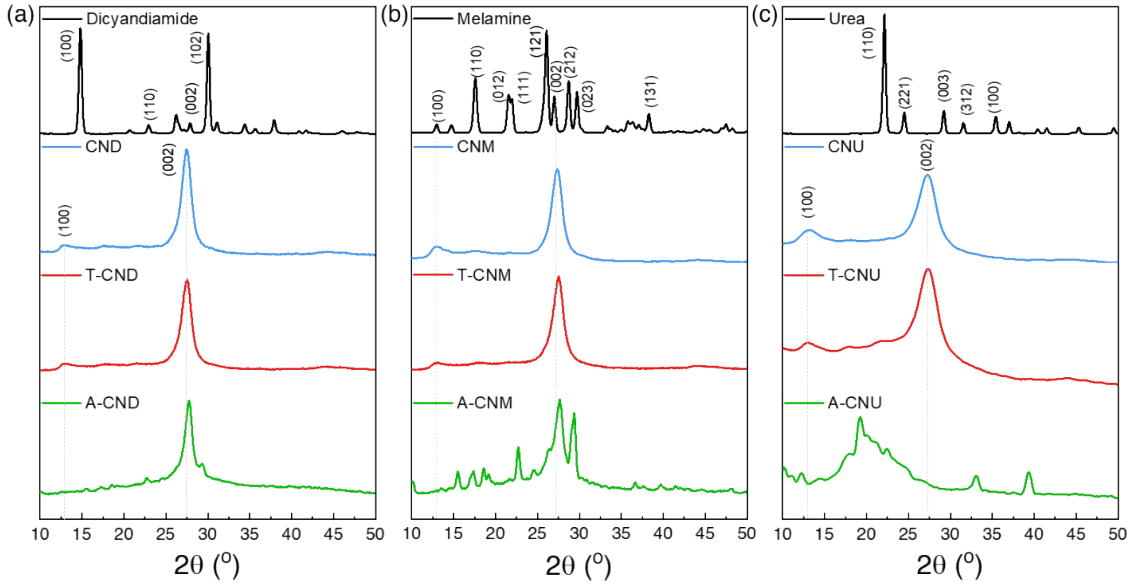

(d)

	Dicyandiamide				Melamine				Urea			
	2θ	d_{100}	2θ	d_{200}	2θ	d_{100}	2θ	d_{200}	2θ	d_{100}	2θ	d_{200}
Bulk	12.8°	0.67 nm	27.4°	0.33 nm	13.0°	0.68 nm	27.3°	0.33 nm	13.1°	0.67 nm	27.3°	0.33 nm
Thermal treatment	12.8°	0.67 nm	27.6°	0.32 nm	12.9°	0.68 nm	27.4°	0.33 nm	13.0°	0.68 nm	27.3°	0.33 nm
Acid treatment	-	-	27.7°	0.32 nm	-	-	27.5°	0.32 nm	12.2°	0.72 nm	-	-

Figure S2: XRD diffractograms for carbon nitrides-based materials using dicyandiamide (a), melamine (b) and urea (c) as precursors and their respective thermal and acid treatments. The bulk samples for all precursors present two reflections centered at ~13° and 27° 2θ, associated with the repetition of the triazine and heptazine subunits and the stacking of the aromatic sheets, respectively. The slight shift observed for the thermal treated samples is associated with an increase in the polymerization level of T-CNM, leading to a reduction in the sp^2 C-N bond length. An increased number of crystalline reflections is observed for all acid-treated samples associated with the presence of defects and the formation of new staking systems due to the rearrangement of the layers during the treatment. The interplanar spacing between the layers (d-spacing) was calculated from the (002) diffraction peaks, and similar results were obtained for all the materials with a d-spacing of approximately 0.3 nm for all samples. However, for A-CNU, with the disappearance of the peak centered at 27° 2θ the calculations were not possible.

3. Fluorescence

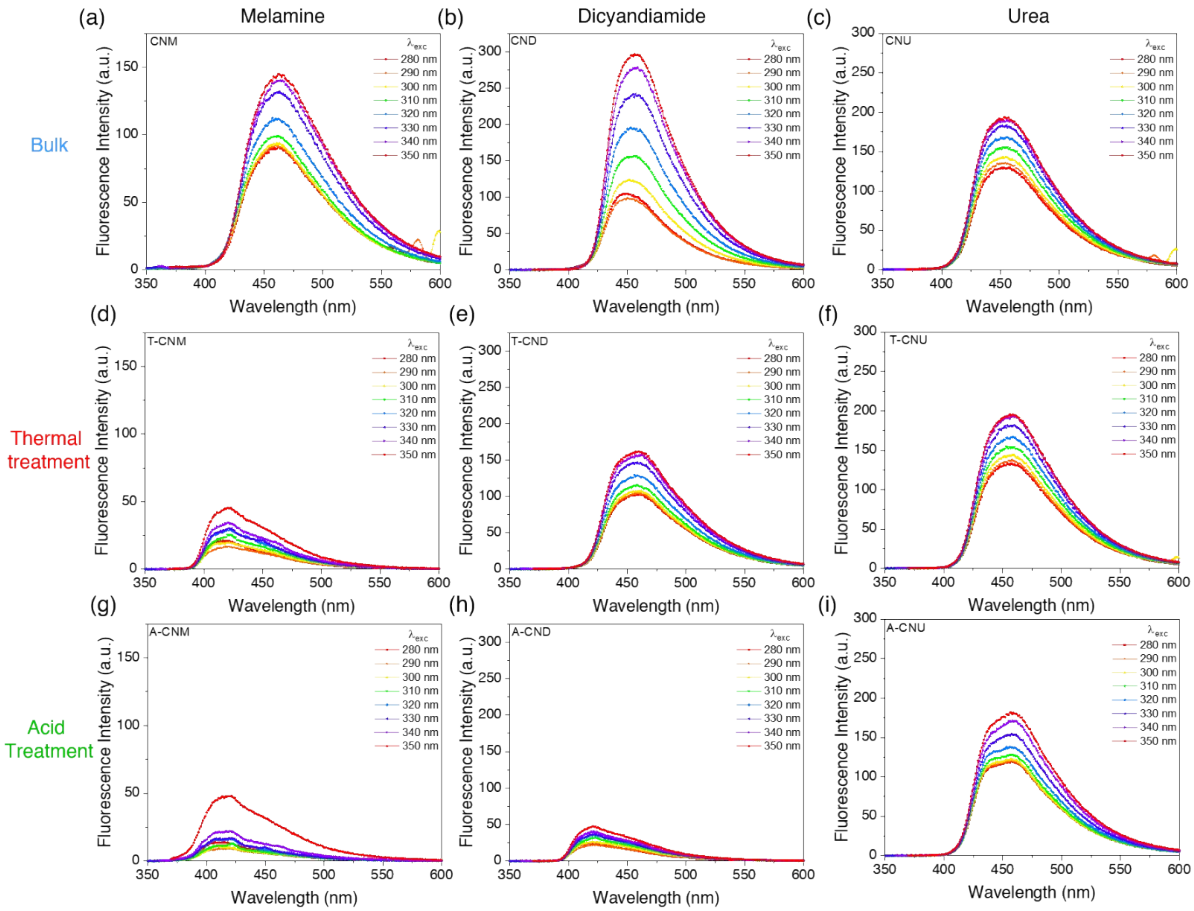

Figure S3: Fluorescence profile under excitation between 280-350 nm for the carbon nitrides synthesized using melamine, dicyandiamide, urea, and their thermal and acid treatments. All bulk samples presented an excitation-independent emission, centered at 460, 456 and 474 nm for CNM (a), CND (b) and CNU (c), respectively. A blue-shift in the maxima was observed for T-CNM (d), T-CND (e), centered at 405, 452, respectively. No changes were observed for T-CNU (f) and A-CNU (i), in which the fluorescence maximum remained centered at 474 nm.

4. Time-resolved Fluorescence

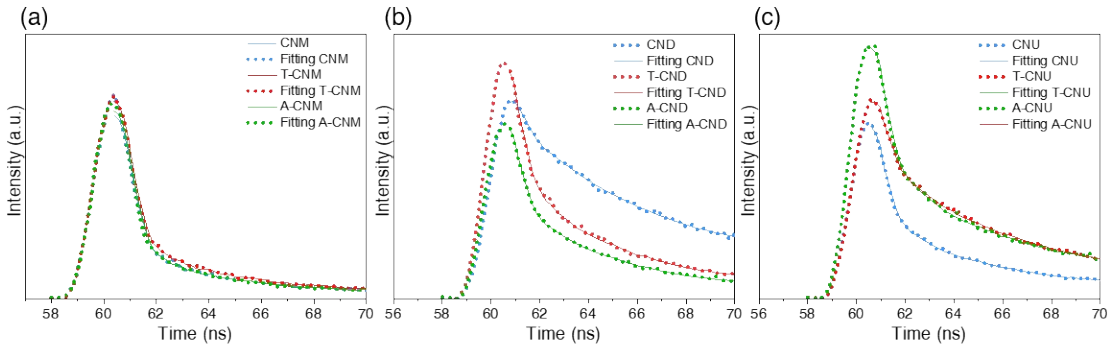

Sample	τ_1 (ns)	Relative %	τ_2 (ns)	Relative %	τ_3 (ns)	Relative %	$\tau_{average}$	χ^2	ϕ (%)
CNM	1.0	69.2	10.4	13.8	2.1	16.9	4.5	1.2	9.3
T-CNM	1.2	39.7	2.6	50.4	0.9	9.9	1.6	1.1	2.7
A-CNM	1.1	25.6	2.9	50.2	0.1	24.1	1.4	1.0	3.4
CND	7.4	73.5	0.1	10.0	1.7	16.5	3.1	1.1	23.3
T-CND	2.9	45.8	0.1	37.8	1.2	16.5	1.4	1.3	11.5
A-CND	4.6	41.9	0.1	38.9	1.6	19.1	2.1	1.0	3.7
CNU	8.2	47.7	0.1	33.8	1.4	18.5	3.2	1.1	14.5
T-CNU	6.0	65.9	0.1	28.6	1.5	15.4	2.5	1.2	17.1
A-CNU	1.4	15.8	0.1	29.5	7.4	54.7	3.0	1.0	14.3

Figure S4: Time resolved fluorescence decay curves for the carbon nitrides using melamine (a), dicyandiamide (b) and urea (c) as precursors. The fitting results for the lifetimes and relative intensities are displayed in the table above along with the fluorescence quantum yield for each sample.

5. Transmission Electronic Microscopy

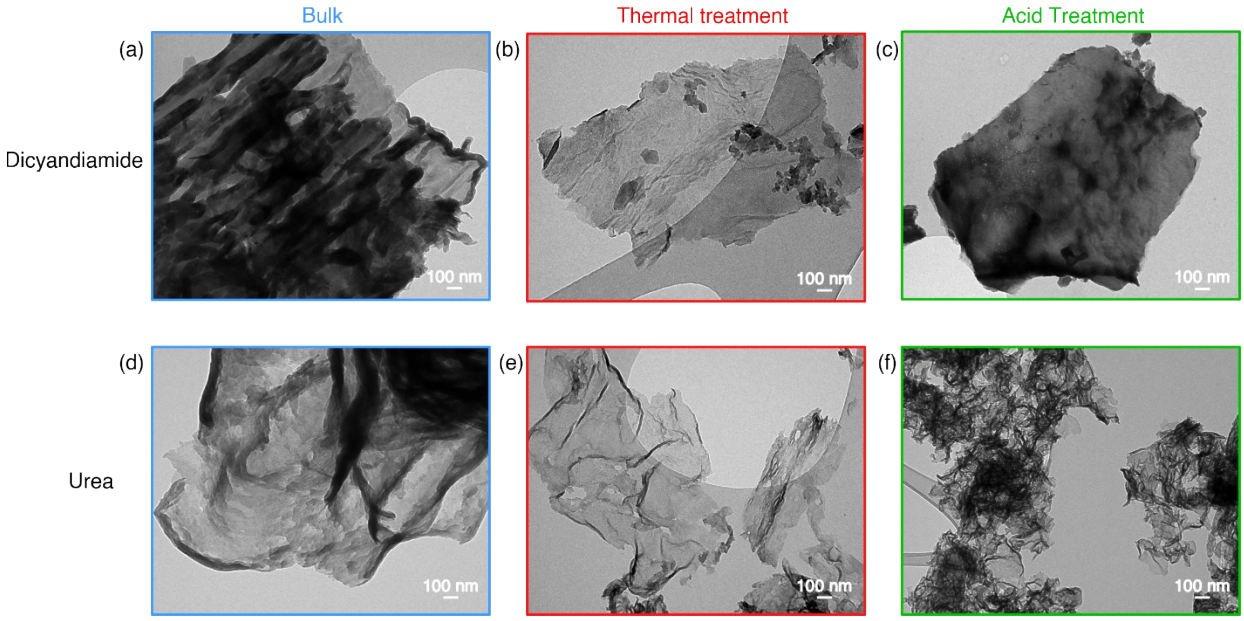

Figure S5: TEM images for the bulk carbon nitrides synthesized from dicyandiamide (a) and urea (d) presenting a lamellar structure with approximately 1 µm in length. However, CNU present reduced thickness when compared to CND and CNM. The thermal treatment of CND and CNU to form T-CND (b) and T-CNU (e) leads to a delamination of the stacked structure when compared to the bulk parent material. The acid treatment of CND lead to the formation of A-CND (c) evidences a thicker structure, similar to the one observed for A-CNM. However, for A-CNU, the acid treatment leads to the formation of defective structures with smaller diameters when compared to the bulk counterpart.

6. Thermogravimetric Analysis

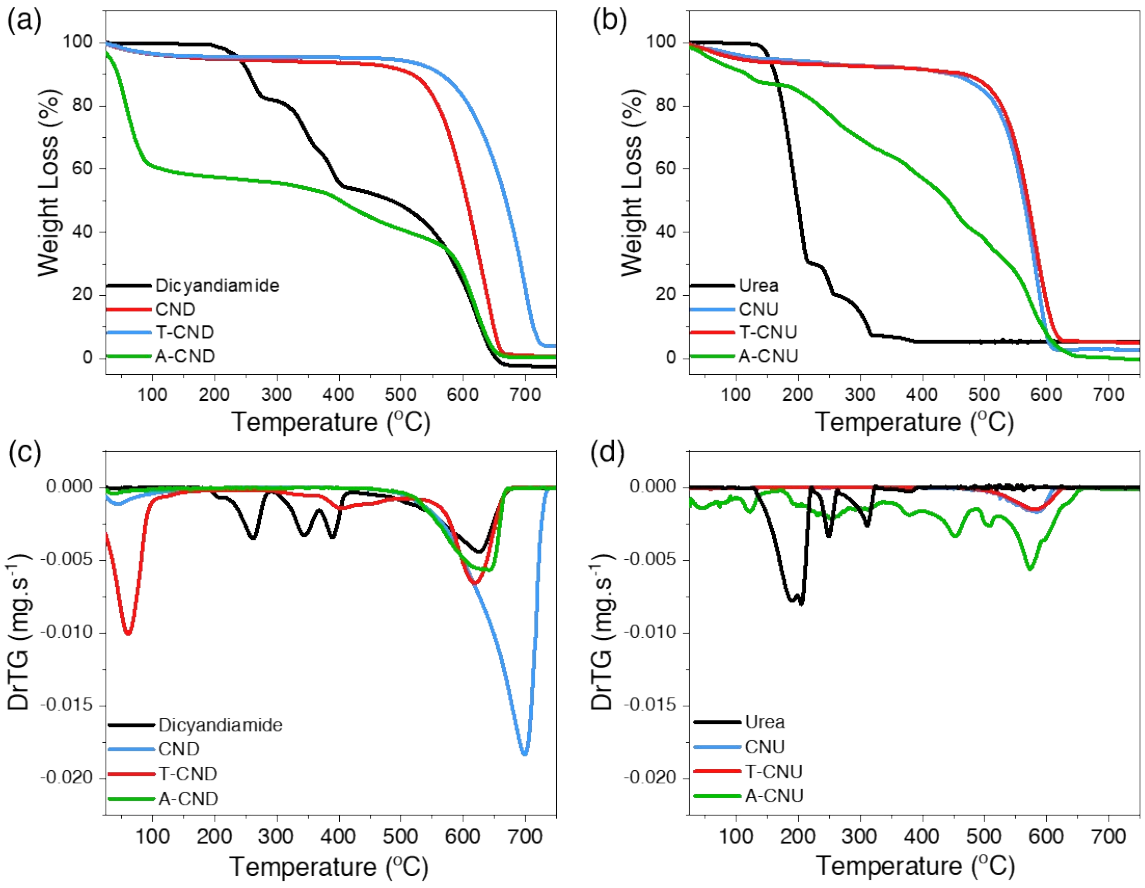

Figure S6: Thermogravimetric analysis of carbon nitrides-based materials synthesized using dicyandiamide (a,c) and urea (b,d) as precursors. CND, T-CND, CNU and T-CNU present a similar initial weight loss ranging from 3-10% associated with the presence of CO_2 and water molecules adsorbed on the surface of the materials. A similar single step decomposition profile is observer for these materials, starting at 575 °C, 541 °C, 466 °C and 467 °C respectively. The acid treated samples, A-CND and A-CNU possess many weight losses events, mostly due to the presence of defects and oxidation of the material during the acid treatment.

7. Elemental Analysis

Sample	C (%)	H (%)	N (%)	C/N atomic
Dicyandiamide	29.0	4.5	67.1	0.50
CND	35.6	1.5	62.5	0.66
T-CND	34.1	1.6	57.3	0.69
A-CND	15.1	1.5	27.0	0.65
Sample	C (%)	H (%)	N (%)	C/N atomic
Urea	20.5	5.6	47.0	0.51
CNU	32.5	1.1	57.7	0.66
T-CNU	33.1	1.2	57.3	0.66
A-CNU	18.8	2.3	35.8	0.61

Figure S7: Elemental analysis of the precursors and the carbon nitride-based materials. The bulk materials, CND and CNU present a similar percentage composition, and consequently the same C/N atomic ratio. The composition of T-CNU remained unaltered; however, a slight change was observed for T-CND when compared to their bulk parent material, mostly due to the increase in the polymerization levels of the materials following the thermal treatment. The acid treatment for both A-CND and A-CNU leads to a considerable decrease in the percentage of C and N, suggesting the incorporation of oxygen moieties and reducing the organization level of the material.

8. Fourier-Transform Infrared Spectroscopy

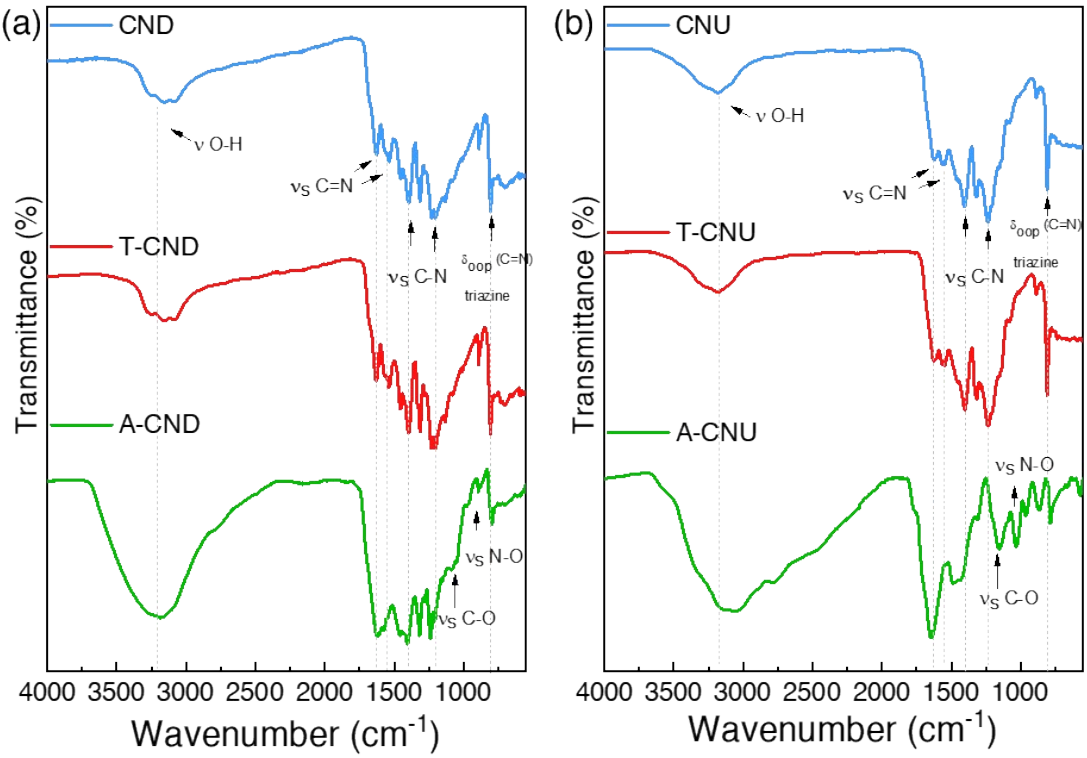

Figure S8: FT-IR spectra for the dicyandiamide (a) and urea (b) bulk materials and their thermal and acid treated samples.

9. Tauc Plot

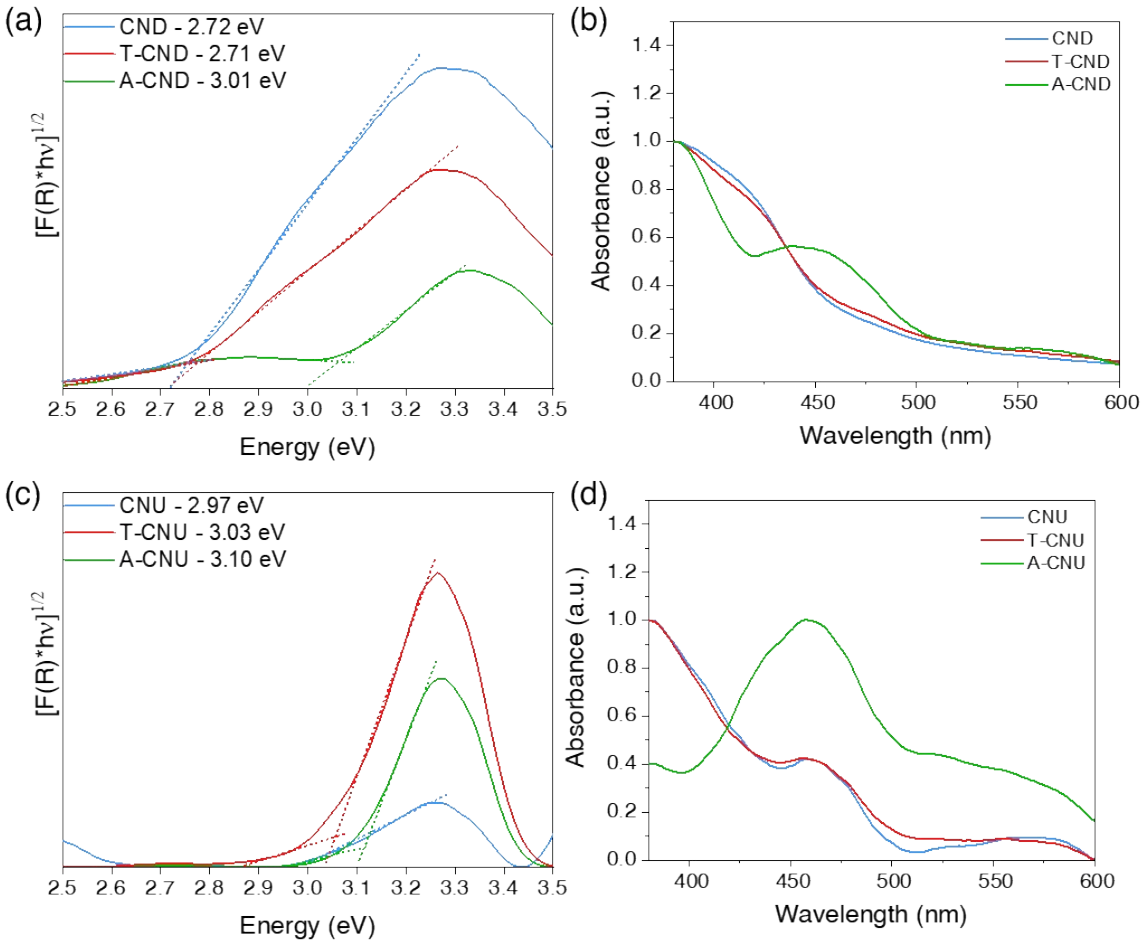

Figure S9: : Tauc plot in reflectance mode and estimated from the intercept of the tangents in $[F(R)(\alpha h\nu)]^{1/2}$ against (hv). The energy gap (E_g) obtained for CND, T-CND and A-CND were 2.72, 2.71 and 3.01 eV, respectively (a). The E_g for CND, T-CNU and A-CNU were 2.97, 3.10 and 3.03 eV, respectively (b). UV-Vis absorbance spectra displaying a broad absorbance bands from 380 to 500 nm for CND, T-CND and A-CND (c), and CNU, T-CNU and A-CNU (d).

10. Fluorescence of the Dicyandiamide and Urea-based Materials

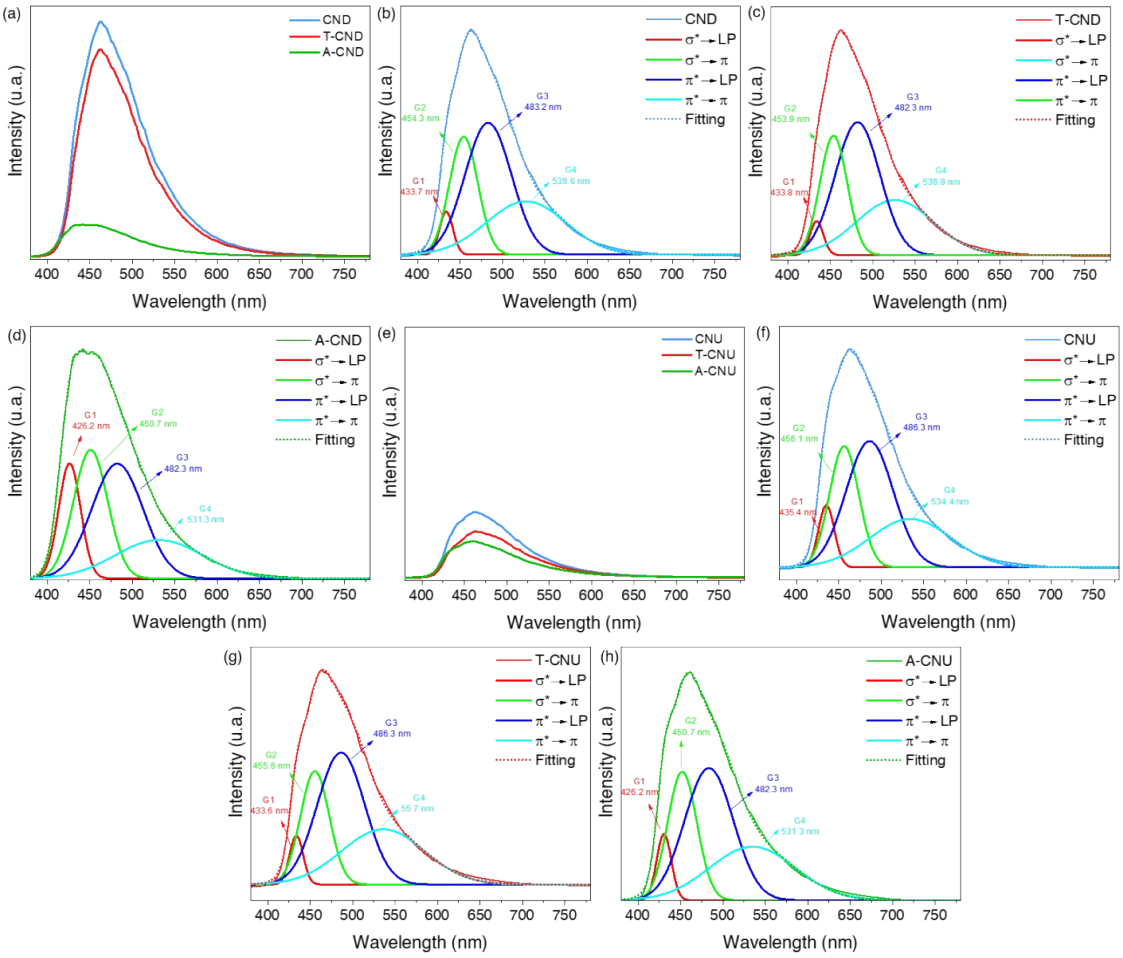

Figure S10: Fluorescence spectra of the samples under an excitation wavelength of 335 nm showed broad emissions centered at 468, 464, and 442 nm, for CNM, T-CNM and A-CNM, respectively (a). For CNU, T-CNU and A-CNU, their emission maxima were centered at approximately 463 nm and remained unchanged after the acid and thermal treatments. The deconvolution of the fluorescence spectra for all were adjusted with four Gaussian fittings: G1, associated with the transition between σ*-LP, G2, ascribed to the transition between σ* and π, G3 corresponding to the pathway of the π*-LP transition and G4 ascribed to the transition between π*-π (b-d and f-h).